



# Multibody Dynamics Modeling of Delta Robot with Experimental Validation

Mohamed Elshami, Mohamed Shehata<sup>(✉)</sup>, Qingshun Bai, and Xuezheng Zhao

Harbin Institute of Technology, Harbin, China  
{mohamed\_elshami, qshbai, zhaozz}@hit.edu.cn,  
mohamed.saleh@stu.hit.edu.cn

**Abstract.** Delta robot is one of the most known parallel systems which possesses high stiffness and accuracy. In order to build a system that endows the robot to perform the desired tasks, an accurate and validate the dynamic model is required. In recent years, researchers have been focused on the construction of serial structured robots. However, few researchers tried to evolve the delta robots in such a system. In this work, the multibody system dynamics (MBS) approach is used to study the kinematics and dynamics of delta robots. A systematic approach is developed based on load assumption due to end-effector movements. The multibody model is constructed using Matlab Symbolic Toolbox. Moreover, D3S-800 is utilized in this study to validate the multibody model. The comparison of experimental data and numerical solution shows a very good agreement and consequently, the multibody model obtained is suitable for parameter identification, control and design optimization of a delta robot system.

**Keywords:** Multibody system dynamics · Delta robot · Matlab symbolic toolbox · Euler parameters

## 1 Introduction

Robot structures possess a good variety of architectural designs adapted to the different industrial and non-industrial operations. While serial manipulators are the most common dominant type of robots in the industry because of their high flexibility. The parallel structured robots provide a good solution to some inconvenient situations of the serial manipulators, such as the situations where the robot is required to resist high loads [10].

Delta robot is one common configuration of parallel robots and what makes the delta robot fascinating is that unlike most of robotic applications which are biologically inspired [14]. Delta robot perception was a mechanical structure design that depended completely on the theory of machines and the correlated relation between the mechanical linkages [5]. Recently, researchers made a lot of effort into modeling, design and control of delta robots using traditional dynamics methods [6, 8]. On the other hand, the multibody system serves as a basis for

many modern models of complex systems and has been applied in many areas of science. The multibody system approach will be used for the dynamic modeling of delta robot in order to increase the efficiency of the system and enhance system control [2]. Also, the multibody model results were verified using actual delta robot system.

The remainder of this study is organized as follows: Sect. 2 introduces the delta robot as a multibody system. In Sect. 3, the constraint's function is expressed, and the model is constructed. Section 4 presents numerical simulation and experimental validation that are followed by the conclusion in Sect. 5.

## 2 Delta Robot as a Multibody System

In this study, D3S-800 delta robot used, in which The robot has three degrees of freedom, the end-effector is free to move in three translational motions along XYZ axes, see Fig. 1. In addition, The manipulator can achieve rotational motion about Z-axis by means of an actuator installed to the fixed base and the rotational motion is transmitted mechanically to the end-effector [3]. The computational model is established to determine the kinematic relationship between the system coordinates. We apply the MBS mathematical calculation process to the incremental robot mechanism and for simplification, the rotational degree of freedom about Z-axis is not considered. Delta robot as a multibody system consists of a fixed base, three arms, six forearms, six rods and an end-effector. To define system bodies, local frames are assigned to delta robot bodies and the base frame is considered the reference coordinate. For simplicity of the computations, the global frame is assigned to the projection of the fixed platform in the same plane enclosing the three points  $a_i$ , which are the positions of revolute joints between the base frame and the active arms [13]. Each single chain shown in Fig. 1b consists of a revolute joint directly actuated by means of an electrical motor. The forearms or the passive arms are connected to the active arms at points  $b_{i1}$  and  $b_{i2}$ , the above two points are connected to the movable platform in points  $c_{i2}$  and  $c_{i1}$  forming the closed loop  $b_{i1}$ ,  $b_{i2}$ ,  $c_{i2}$  and  $c_{i1}$ . Another closed-loop  $s_{i1}$ ,  $s_{i2}$ ,  $t_{i2}$  and  $t_{i1}$  formed by the connecting rods which functions are to maintain the connectivity of the spherical joints and to prevent the forearms from the undesired rotations about their longitudinal axis. At the initial home position, an end-effector frame is collinear with the Z-axis of the reference coordinate.

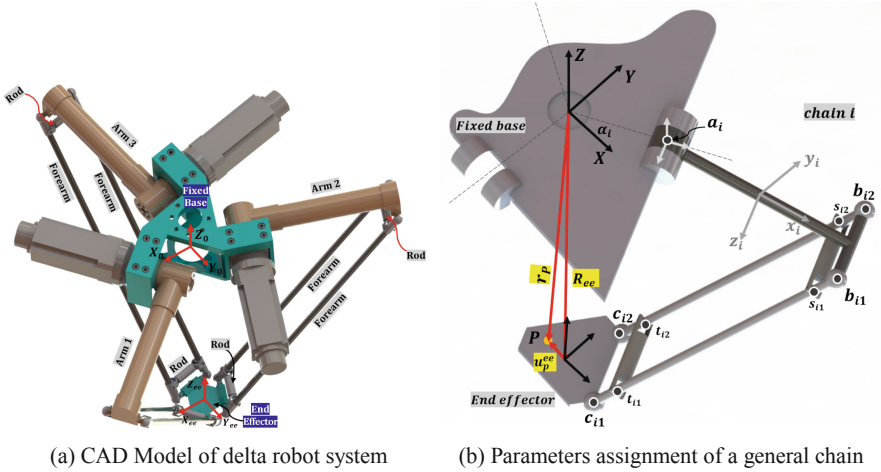


Fig. 1. Multibody model of delta robot system

### 3 Mathematical Model of Delta Robot

The model of the delta robot shown in Fig. 1a, can be constructed, without loss of generality, as shown in Table 1 for the first chain. Let the contact point  $\mathbf{P}$  be located on the end-effector frame. The system of generalized coordinates is denoted by  $\mathbf{q}$  and can define function in Euler angles  $\phi, \theta$  and  $\psi$  [4]. To avoid a singularity during simulation, the three Euler angles will convert to four Euler parameters  $[q_0^1 \ q_1^1 \ q_2^1 \ q_3^1]$  [12]. The generalized coordinates of the fixed base including translation and orientation are defined as:

$$\mathbf{q}^1 = [x^1 \ y^1 \ z^1 \ q_0^1 \ q_1^1 \ q_2^1 \ q_3^1] \tag{1}$$

The global portion vector of that point can be expressed as:

$$\mathbf{r}^i = \mathbf{R}^i + \mathbf{A}^i \bar{\mathbf{u}}_p^i \tag{2}$$

Table 1. Components of Delta robot system

Joint number	Joint type	Body(i)	Body(j)
1	Fixed	Fixed Base	Ground
2	Revolute	Arm	Fixed Base
3	Spherical	Forearm1	Arm
4	Revolute	Rod1	Forearm1
5	Revolute	Forearm2	Rod1
6	Revolute	Rod2	Forearm2
7	Spherical	Forearm1	End-effector

where  $\mathbf{r}^i$ , is the global position of an arbitrary point,  $\mathbf{R}^i$ , is the global position of the origin of the end-effector coordinate system, and  $\mathbf{A}^i$  is the transformation matrix function on the generalized coordinates. It is clear from Eq. (2) that the global position vector of an arbitrary point on the body coordinate system can be written in terms of the rotational coordinate of the body, as well as the translation of the frame-origin of the body. In order to avoid singularities, Euler parameters are used to describe the orientation of the system bodies and result coordinates can be converted back to cartesian coordinates [11]. The constraints function of delta robot can be obtained using multibody constraints equation of Rigid, Revolute and Spherical joints. Equation 3 illustrates constraints equations of rigid joint between fixed base and ground.

$$\mathbf{C}^1_{(\mathbf{q}^g, \mathbf{q}^1, t)} = \begin{bmatrix} x^1 \\ y^1 \\ z^1 \\ 1 - 2(q_2^1)^2 - 2q_0^1 q_2^1 - 2q_1^1 q_3^1 - 2(q_1^1)^2 \\ 2(q_1^1)^2 + 2(q_2^1)^2 - 2q_0^1 q_1^1 - 2q_1^1 q_3^1 - 1 \\ 2(q_1^1)^2 + 2(q_2^1)^2 - 2q_0^1 q_2^1 - 2q_1^1 q_3^1 - 1 \\ (q_0^1)^2 + (q_1^1)^2 + (q_2^1)^2 + (q_3^1)^2 - 1 \end{bmatrix} = 0 \quad (3)$$

where  $\mathbf{q}^g$  is generalized coordinate vector for ground and it equal zero and  $\mathbf{q}^1$  is generalized coordinate vector of the fixed base. Figure 2a shows revolute joint between Arm1 and fixed base. The constraints equations of revolute joints between Arm1 and fixed base can be written as:

$$\mathbf{C}^2_{(\mathbf{q}^1, \mathbf{q}^2, t)} = \begin{bmatrix} x^1 - x^2 \\ y^1 - y^2 \\ z^1 - z^2 \\ 1 - 2(q_2^1)^2 - 2q_0^1 q_2^1 - 2q_1^1 q_3^1 - 2(q_1^1)^2 \\ 2(q_1^1)^2 + 2(q_2^1)^2 - 2q_0^1 q_1^1 - 2q_1^1 q_3^1 - 1 \\ (q_0^2)^2 + (q_1^2)^2 + (q_2^2)^2 + (q_3^2)^2 - 1 \end{bmatrix} = 0 \quad (4)$$

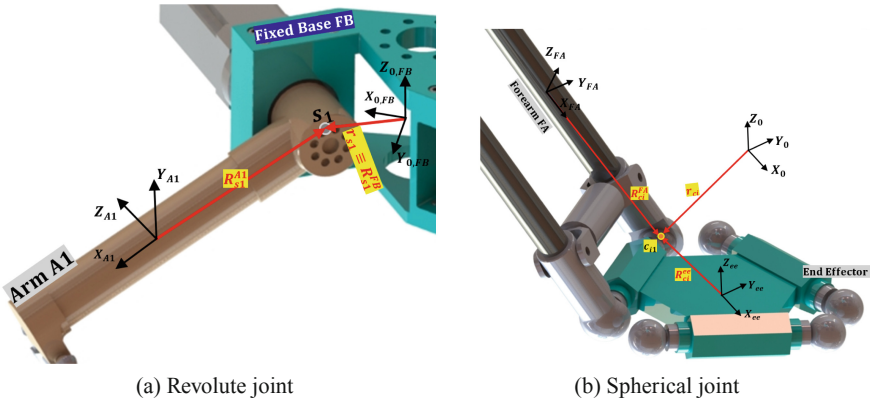


Fig. 2. Multibody joint constraints

where generalized coordinates of Arm1 is define as  $\mathbf{q}^2 = [x^2 y^2 z^2 q_0^2 q_1^2 q_2^2 q_3^2]$ . Figure 2b shows spherical joint between the forearm and end-effector. The constraints equation of spherical joints between Forearam1 and Arm can be written function on translation constraints as:

$$\mathbf{C}_{(\mathbf{q}^2, \mathbf{q}^3, t)}^3 = \begin{bmatrix} x^2 - x^3 \\ y^2 - y^3 \\ z^2 - z^3 \end{bmatrix} = 0 \quad (5)$$

Constraints equations for other joints can be defined similarly to spherical and revolute joints. The dynamic equations that govern the motion of system bodies can be systematically obtained using Lagrange formulation as [1]:

$$\begin{bmatrix} \mathbf{M} & \mathbf{C}_q^T \\ \mathbf{C}_q & \mathbf{0} \end{bmatrix} \begin{bmatrix} \ddot{\mathbf{q}} \\ \lambda \end{bmatrix} = \begin{bmatrix} \mathbf{Q} \\ \mathbf{Q}_d \end{bmatrix} \quad (6)$$

where  $\mathbf{M}$  is the system mass matrix,  $\mathbf{C}_q$  is the system Jacobian matrix  $\mathbf{C}_q = \frac{\partial \mathbf{C}(q,t)}{\partial q}$ ,  $\lambda$  the vector of Lagrange multipliers and  $\mathbf{Q}_d$  is a vector absorb terms that are quadratic in the velocity and  $\mathbf{Q}$  is a vector of external applied forces and can be written as:

$$\mathbf{Q} = \begin{bmatrix} \mathbf{Q}_{exR}^i \\ \mathbf{Q}_{ex\theta}^i \end{bmatrix} = \begin{bmatrix} F^i \\ \mathbf{G}^{iT} M^i \end{bmatrix} = \begin{bmatrix} F^i \\ \bar{\mathbf{G}}^{iT} \bar{M}^i \end{bmatrix} \quad (7)$$

where  $\mathbf{Q}_{exR}^i$  is the force associated with the translation coordinates and  $\mathbf{Q}_{ex\theta}^i$  is the force associated with the orientation coordinates.  $F^i$  and  $M^i$  are the forces and moment vectors defined in the local coordinate system of the body. The matrix  $\bar{\mathbf{G}}^i$  is define function on Euler parameter generalized coordinates and can be written as:

$$\bar{\mathbf{G}}^i = 2 * \begin{bmatrix} -q_1 & q_0 & q_3 & -q_2 \\ -q_2 & -q_3 & q_0 & q_1 \\ -q_3 & q_2 & -q_1 & q_0 \end{bmatrix} \quad (8)$$

Equation of motion Eq. 6 yields a system of differential algebraic equations [7]. A set of initial parameters including positions and velocities from the CAD model are used to start the dynamic simulation [4]. The vector  $\ddot{\mathbf{q}}$  can be integrated in order to determine the coordinates and velocities. The vector  $\lambda$  can be used to determine the generalized reaction forces that can be used to establish optimization of the design process. Because the direct numerical solution of differential algebraic equations associated with the constrained dynamics of a multibody system poses several computational difficulties, a post-stabilization process is used to brings the solution back to the invariant manifold.

## 4 Numerical Simulation and Experimental Validation

In this section, Multibody model results are represented and compared with experimental data. A mathematical model of the delta robot is developed

by applying multibody dynamics theory based on the Lagrange formulation described in the previous section. Kinematics results include system displacements and dynamic results included reaction forces and torques acting on delta robot bodies are computed. The parameters of the D3S-800 delta system are provided in Table 2. The fixed base radius is the radius of a circle that passes through the three points of the revolute joints of arms, while the radius of the movable platform that carries end-effector is the radius of a circle that passes through the six points of the lower spherical joints between the platform and the forearms. By applying an initial motion of 100 mm/s with  $45^\circ$  in XY-plane on the end-effector and keep the distance between the fixed frame and end-effector frame 847 mm in the negative Z direction, the corresponding structural displacement of the delta robot links can be obtained. The simulation is performed using Matlab and Adams-Bashforth-Moulton (ODE113) as the numerical integrator for 5s. Figure 3a shows the constraints violation due to the revolute joint between the arm and fixed base [9]. The violation does not exceed  $3 \times 10^{-13}$  which indicates the computational efficiency of the multibody system model. Noted that, the constraint equation C6 is an Euler parameter constraint that must be added in case of using Euler parameter to define system generalized coordinates. By integrating the system accelerations forward, the system bodies velocities and configurations are computed. According to initial input, the end-effector displacement in XY-plane and the distances in Z-direction constant, see Fig. 3b. Reactions forces acting on deferent bodies of delta robot system are computed from the MBS model as a function of generalized coordinates using Lagrange multipliers. Figures 4 show reaction forces acting on a fixed base including translation forces and moments. As shown in Fig. 4a, the reaction force in Z-direction is due to the wight. Likewise, other system body's reaction forces can be computed. Experimental work is carried out in order to validate the dynamic model of the delta robot. As shown in Fig. 5, the D3S-800 delta robot system consists of robot arms, motors, control unite, encoder and programming unite. Figure 6 shows the comparisons between the output rotor velocity of the MBS model and the experimental data. Since the multibody model and experiment data have similar results, the MBS model is accurate and can be useful for establishing the optimization process of delta robot system design and control.

**Table 2.** Delta robot parameters employed in the numerical simulation

Components	Dimensions (mm)	Mass (kg)	$I_{xx}(Kg \cdot m^2)$	$I_{yy}(Kg \cdot m^2)$	$I_{zz}(Kg \cdot m^2)$
Fixed base	R = 125	30	0.52202	0.52202	0.88497
Arm	L = 370	6.2	0.00510	0.12448	0.125448
Forearm	L = 960	1.65	0.13940	0.00006	0.13940
Connecting rod	L = 95	0.2	0.0000147	0.000101	0.000101
End-effector	r = 62	0.9	0.001031	0.001031	0.002019

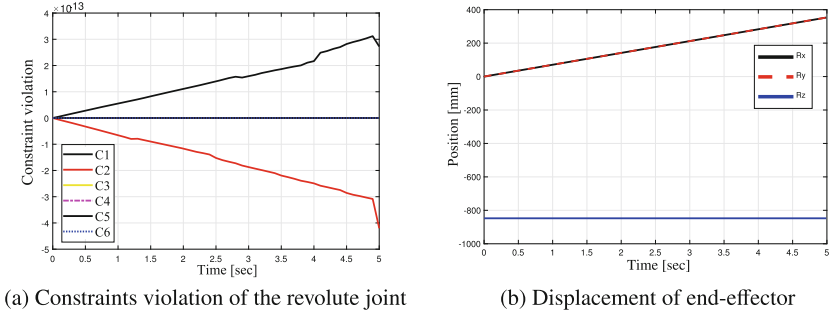


Fig. 3. Constraints violation and global position of the point P

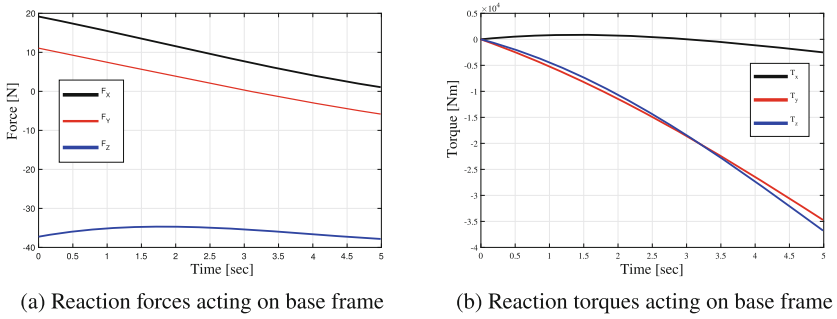


Fig. 4. Reaction forces due to revolute joint

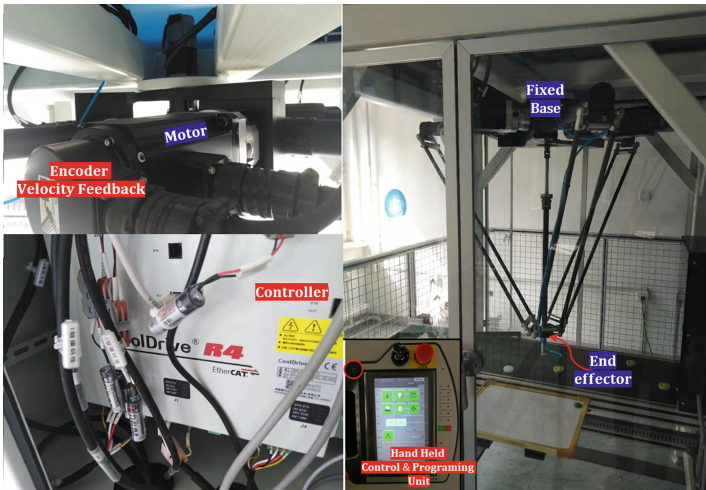
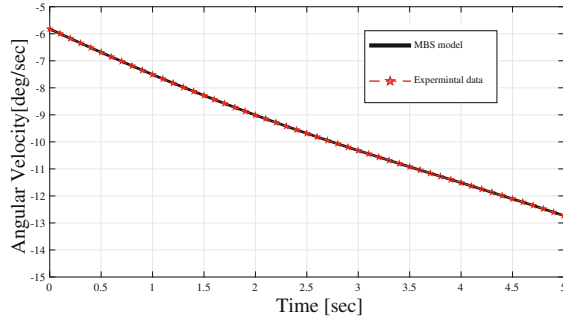


Fig. 5. D3S-800 delta robot system



**Fig. 6.** Angular speed of motor 1

## 5 Conclusion

In this paper, an efficient modeling procedure for the delta robot system is developed based on Multibody system dynamics. The symbolic and computational work have been carried out using Matlab. The symbolic derivation is carried out and the explicit equations of motion of the delta robot have been derived. The solution of the equations of motion involves the system coordinates and the associated Lagrange multipliers as well. The paper describes an experimental test-rig of the D3S-800 delta robot system in front of end-effector movement and the measured motors speed is collected and compared with the multibody model. The comparison shows a very good agreement which encourages the enhancement of the model by examining unconventional operating conditions. Moreover, Lagrange multipliers can be used to estimate the generalized reaction forces which can be utilized in the optimization of delta robot design. In going and future work, multibody model will be used for parameters identification and design optimization of the delta robot.

**Acknowledgement.** This research was supported by National Natural Science Foundation of China (Grant No.71175102 and 52075129).

## References

1. Bai, Q., Shehata, M., Nada, A.: Efficient modeling procedure of novel grating tiling device using multibody system approach. In: Pucheta, M., Cardona, A., Preidikman, S., Hecker, R. (eds.) *MuSMe 2021. MMS*, vol. 94, pp. 168–176. Springer, Cham (2021). [https://doi.org/10.1007/978-3-030-60372-4\\_19](https://doi.org/10.1007/978-3-030-60372-4_19)
2. Barreto, J.P., Corves, B.: Matching the free-vibration response of a delta robot with pick-and-place tasks using multi-body simulation. In: 2018 IEEE 14th International Conference on Automation Science and Engineering (CASE), pp. 1487–1492. IEEE (2018)
3. Chang, Z., Ali, R.A., Ren, P., Zhang, G., Wu, P.: Dynamics and vibration analysis of delta robot. In: 5th International Conference on Information Engineering for Mechanics and Materials, pp. 1408–1417. Atlantis Press (2015)

4. Flores, P.: Concepts and Formulations for Spatial Multibody Dynamics. Springer, Heidelberg (2015)
5. Fumagalli, A., Masarati, P.: Real-time inverse dynamics control of parallel manipulators using general-purpose multibody software. *Multibody Syst. Dyn.* **22**(1), 47–68 (2009)
6. Hamdoun, O., Bakkali, L.E., Baghli, F.Z.: Analysis and optimum kinematic design of a parallel robot. *Procedia Eng.* **181**, 214–220 (2017). <https://doi.org/10.1016/j.proeng.2017.02.374>. <https://www.sciencedirect.com/science/article/pii/S1877705817309578>. 10th International Conference Interdisciplinarity in Engineering, INTER-ENG 2016, Tirgu Mures, Romania, 6–7 October 2016
7. Kunkel, P., Mehrmann, V.: *Differential-Algebraic Equations: Analysis and Numerical Solution*, vol. 2. European Mathematical Society (2006) <https://doi.org/10.1016/j.proeng.2017.02.374>. URL <https://www.sciencedirect.com/science/article/pii/S1877705817309578>
8. Lenarcic, J., Wenger, P.: *Advances in Robot Kinematics: Analysis and Design*. Springer, Heidelberg (2008)
9. Marques, F., Souto, A.P., Flores, P.: On the constraints violation in forward dynamics of multibody systems. *Multibody Syst. Dyn.* **39**(4), 385–419 (2016). <https://doi.org/10.1007/s11044-016-9530-y>
10. Merlet, J.P.: *Parallel Robots*, vol. 128. Springer, Heidelberg (2005)
11. Pappalardo, C.M., Guida, D.: On the use of two-dimensional Euler parameters for the dynamic simulation of planar rigid multibody systems. *Arch. Appl. Mech.* **87**(10), 1647–1665 (2017)
12. Shabana, A.A.: Euler parameters kinetic singularity. *Proc. Inst. Mech. Eng. Part K: J. Multi-body Dyn.* **228**(3), 307–313 (2014)
13. Stock, M., Miller, K.: Optimal kinematic design of spatial parallel manipulators: application to linear delta robot. *J. Mech. Des.* **125**(2), 292–301 (2003)
14. Yang, X., Feng, Z., Liu, C., Ren, X.: A geometric method for kinematics of delta robot and its path tracking control. In: 2014 14th International Conference on Control, Automation and Systems (ICCAS 2014), pp. 509–514. IEEE (2014)